Water Resources Management (2026) 40:124
https://doi.org/10.1007/s11269-026-04500-x

Urban Flood Vulnerability, Economic Loss, Functionality Loss, and Restoration Modeling in Built Environment: Probabilistic Model Formulation and Application in a Mixed Formal and Informal Setting

Vishnu Prasad Pandey[1,2] · Pradhumna Joshi[1] · Rabindra Adhikari[3] · Bhesh Raj Thapa[4] · Sabin Dangol[1] · Ashish Devkota[1] · Aayush Gautam[1] · Giovanni Forte[5] · Dipendra Gautam[6]

Received: 22 April 2025 / Accepted: 9 January 2026

Abstract
Flooding is well recognized as one of the most destructive natural disasters, often leading to heavy losses of lives, property, and economy. Flood impacts are often presented in terms of flood vulnerability/fragility functions considering univariate intensity measures. However, flooding duration also plays an instrumental role in physical damage, functionality loss, and economic losses. This prompts the development of multivariate flood vulnerability and loss models; however, such models are not available in the existing literature to the best of our knowledge. To address this gap, we develop multivariate and univariate flood vulnerability models, economic loss models, and restoration models for Reinforced Concrete (RC), masonry, steel, and semi-permanent buildings. Similar models are also developed for agricultural land using actual damage/loss data. Bivariate models considering inundation depth and inundation duration are developed using response surface method, whereas several univariate vulnerability and loss models are also presented. The models are interpreted together with the outcomes of two-dimensional flood hazard analysis to outline and exemplify probabilistic flooding scenarios and likely consequences. The sum of observations highlights that although physical damage can be limited in building structures, considerable functionality and economic losses will be inevitable due to urban flooding.

Keywords Urban flooding · Flood vulnerability · Functionality loss · Vulnerability surface · Economic loss · Restoration function · Probabilistic modeling

1 Introduction

Flooding is known to impact built environment as exemplified by the damage and loss statistics incurred during many historical events worldwide. Under the changing climate, ever increasing weather extremes are aggravating flooding scenarios globally. Neverthe-

Extended author information available on the last page of the article

less, flooding is one of the most devastating events resulting in fatalities, injuries, physical losses, and economic consequences. Almost 23% of the global population is estimated to be exposed to a 100-year return period flood, of which 89% of the affected population is from low-to-middle income countries (Rentschler et al. 2022). The World Bank estimates the direct physical losses attributed to flooding would be over US$ 300 billion per annum (Bangalore et al. 2017). It is also evident that south and southeast Asia observes most frequent and devastating flooding events. It is also worth noting that the region does not have adequate resilient measures and infrastructures to cope with the frequent flood occurrences. Thus, damage and losses are often aggravated due to the lack of flood resilience infrastructures and initiatives. When an entity is damaged by flooding, it incurs economic consequences as well as functionality disruption. When a system is disrupted, it requires restoration to regain normal functionality, which incurs investment. Thus, flooding causes physical damage to an entity, which leads to economic consequences and functionality losses; both of these prompt restoration, which is again hinged with the integrity of the system exposed to flooding or any external force.

Large amount of insurance should be covered by the agencies and the government authorities after almost every flood. Even in the absence of flooding insurance policies, government subsidies are often allocated in Nepal. In this case, budget rerouting is required, which results in secondary consequences such as derailed infrastructure development, and so on. For reliable insurance premium planning, vulnerability and loss models play instrumental role by providing the level or extent of likely damage and corresponding insurance amount conditioned to the replacement values. Thus, the need for studies pertaining to flood vulnerability, loss, and functionality restoration are gaining momentum lately. Most of the existing studies use qualitative dissemination of flood vulnerability based on built environment characteristics (Cheng et al. 2024; de Moraes and Gonçalves 2024; Jang et al. 2021; Panagiotou et al. 2025). These models provide comparative intensity and susceptibility, but not quantitative loss or damage ratios.

Flood damage, vulnerability, and loss are accounted for in field assessments following major flood events. The empirical data collected after major flood events is proven to be instrumental in constructing flood vulnerability models. Flood damage mechanisms in various structures, infrastructures, and lifelines are reported after major flood events from across the world (see e.g. Santo et al. 2016; Santangelo et al. 2021; Santo et al. 2018; Gautam and Dong 2018; Gautam et al. 2023; Thapa et al. 2020). Using empirical damage data, flood vulnerability/fragility functions are developed for various components of the built environment, ranging from residential buildings to infrastructures. Precisely, residential buildings have remained the prime focus of empirical flood vulnerability analysis (Karagiorgos et al. 2016; Papathoma-Köhle et al. 2017; Fuchs et al. 2019a, b; Papathoma-Köhle et al. 2022; Thapa et al. 2020; Gautam et al. 2023; Arrighi et al. 2020; De Risi et al. 2020). However, limited attention is paid for nonstructural components exposed to flooding (Forte et al. 2025). Despite empirical models, numerical modeling(Gautam et al. 2023) and experimental campaigns(Sturm et al. 2018) are also used in flood vulnerability modeling. Using flood vulnerability models, example applications and probabilistic scenario risk assessments have been executed in many parts of the world (see e.g. Totschnig and Fuchs 2013; Taramelli et al. 2022; Mascheri et al. 2024). Although actual empirical loss/damage data are more trustworthy if bias is constrained, a major drawback in univariate flood vulnerability mod-

els lies in terms of explicit representation of flooding duration and its impacts. Damage to structures and infrastructures is fundamentally attributed to flow velocity, inundation depth, and flooding duration.

Although inundation depth is the most widely used intensity measure (IM) in univariate flood vulnerability analysis (Pistrika et al. 2014), it is imperative to note that this IM is not exhaustive. Supporting evidence was provided by Gautam et al. (2023), using numerical modeling. Inundation depth alone cannot explain the overall damage/loss extent as gradual and aggregated damage is the characteristic damage during flooding, rather than an impulse response type mechanism. To this end, Molinari et al. (2020) highlighted the need for multivariate vulnerability models for more realistic disseminations. Multivariate vulnerability and loss models have been deemed necessary for quite some time now, but the key challenge remains in terms of the availability of multiple IMs in databases. It is because most of the post-flood surveys fail to report flood intensity, duration, and damage extent, simultaneously. Thus, there exists an opportunity to refine flood vulnerability models for structures, infrastructures, and lifelines, and any other assets considering multivariate modeling. Furthermore, almost all flood risk assessment approaches and applications focus only on vulnerability aspect only. On the other hand, multivariate loss, functionality loss, and restoration models are either sparse or absent otherwise. Not just physical vulnerability can explain the broad spectrum of flood risk, instead economic loss or flood loss incurred to physical damage, and functionality loss, and restoration are pivotal. It is because most of the frequent floods do not necessarily incur damage but rather cause functionality loss (disruption) and claim economic consequences only. To the best of our knowledge, limited attention is paid to these dimensions. Although local, rather than global models, are considered more realistic vulnerability models (Molinari et al. 2020; Gautam, Fabbrocino, and Santucci de Magistris 2018), attention toward flood vulnerability models even in the areas with frequent flooding is still insufficient because most of the structures, infrastructures, and lifelines do not have flood vulnerability, flood loss, and functionality restoration models.

Flood risk zonation/mapping is a highly interdisciplinary field involving hydrology, hydraulic engineering, social engineering, structural engineering, and several other fields. Thus, transdisciplinary approach is required to depict realistic flood susceptibility analysis. Otherwise, most of the outcomes would not be coordinated and thus the models do not fulfill the requirements of integrated transdisciplinary studies. Notably, only a few studies adopted transdisciplinary approach in flood risk studies (see e.g. Thapa et al. 2020; Amirmoradi and Shokoohi 2024). For pragmatic considerations in terms of usability and translatability of the scattered domains, transdisciplinary efforts are required. Aiming to contribute to this dimension, the present study develops flood vulnerability, loss, and functionality restoration models for various components within the built environment. Univariate and multivariate vulnerability and loss models are developed for structures and built environment. Also, preliminary functionality restoration models are developed. The models are implemented to depict flood hazard, vulnerability, and loss scenarios in Bagmati River, Kathmandu, Nepal. The originality of the present contribution lies in the development of bivariate flood vulnerability models and loss models for a highly flood prone region. Four dominant construction systems are incorporated to develop some of the earliest models in this domain.

2 Materials and Methods

A methodological framework to assess flood vulnerability, loss, and functionality restoration modeling is shown in Fig. 1. The three major attributes of the methodological framework are the data, model, and application. In order to execute the proposed methodology, taxonomy formulation is the first step. Flood vulnerability, loss, and functionality restoration require well defined taxonomy. This is the key step to minimize aleatoric uncertainties as well since different structures and components behave differently under flood loading. RC buildings, brick masonry buildings, steel buildings, semi-permanent buildings, agricultural land, electric poles with transformer, electric poles without transformer, paved road, unpaved road, retaining structures, RC bridge, steel bridge, and foot trail bridge were considered as structure and infrastructure classes during taxonomy formulation. In order to develop flood vulnerability, flood loss, and functionality restoration models, two extensive survey campaigns were conducted after the September 2024 and October 2024 floods that occurred in Kathmandu Valley, Nepal. Kathmandu Valley observes devastating floods almost every year, so the data and models basically represent a highly flood prone area. Field study questionnaires were developed to capture inundation depth, damage extent, flooding duration, loss amount, functionality loss and restoration time, among others. As shown in Fig. 1, damage incurred to the entity, depth of inundation in meter, and inundation duration in hour were the major information collected to construct flood vulnerability models. Meanwhile, supporting evidence such as pictorial representation and explanations regarding construction system were also noted during the field survey. We collected 26 data pairs for RC, 26 data pairs for masonry, 8 data pairs for steel, 22 data pairs for semi-permanent buildings, and 11 data pairs for agri-

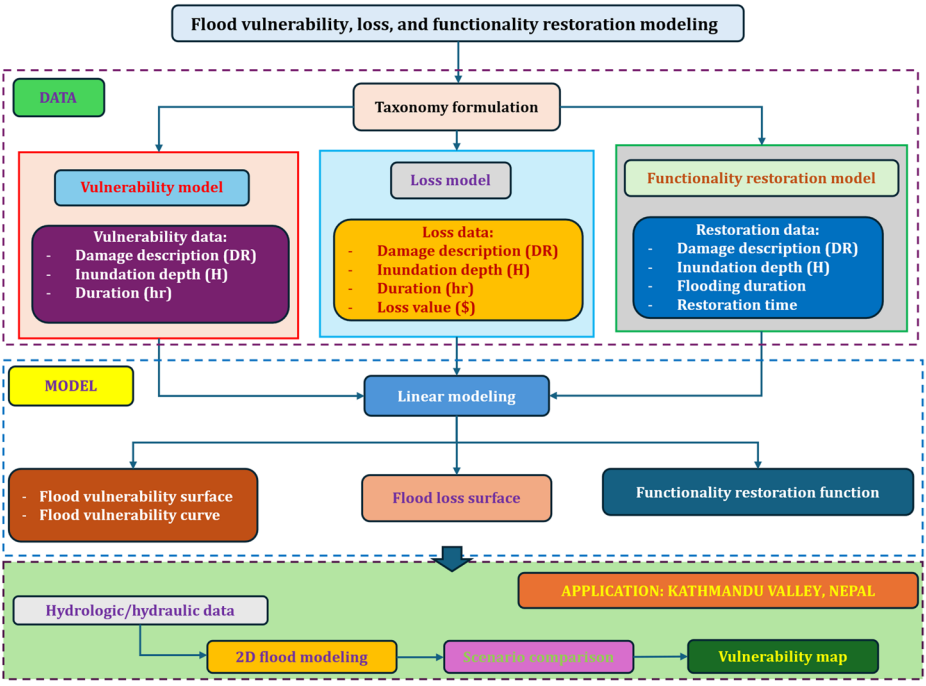

Fig. 1 Methodological framework for flood vulnerability, loss, and functionality restoration modeling

cultural land. Maximum inundation for RC, masonry, steel, semi-permanent buildings, and agricultural land was respectively 2.5 m, 2.5 m, 1.95 m, 1.65 m, and 0.85 m. The data were collected from the areas affected by the 2024 flooding and all entities along the flood course were surveyed. Thus, no sampling rules or exclusion criteria were during the field survey. On the other hand, we were not able to get enough data for electric poles, bridges, and other entities; thus, vulnerability models for these entities have not been developed. Using the dataset, bivariate flood vulnerability surfaces and univariate flood vulnerability curves are fitted. We used Response Surface Method (RSM) to generate vulnerability surfaces, whereas statistical fitting is done to create univariate vulnerability models. Further dissection of data and opted model is presented in the results section. The RSM method allows creation of vulnerability surfaces, as well as captures the interaction between the independent variables. The interaction dimension is not usually accounted for in normal multivariate regression. For a scenario such as flooding in which both inundation depth and duration act side by side to result in damage/loss, RSM suits better than normal multivariate regression. It is worth noting that flood vulnerability surfaces have not been proposed yet to the best of our knowledge. Loss models are generated using the same approach but the dependent variable, loss value, is conditioned to damage ratio (DR) and inundation depth (H). DR is defined as the ratio between the loss value incurred by the flood event to the total restoration cost. In many cases, there will be only content loss rather than physical damage to the entity under consideration; however, we use the same approach to quantify DR even when the loss is incurred to nonstructural components or contents. Equivalent DR is assigned in each case based on qualitative description of damage incurred to the entity under consideration. Inundation depth is directly measured by a measuring tape, demarcating the high flood level (HFL). Since inundation duration (T) is also an important parameter to characterize loss and damage, we recorded the parameter through interviews. Subjective bias can occur when translating qualitative descriptions to DR and also in the duration provided by homeowners. However, we have not considered any measure to treat the likely biases. For functionality restoration modeling, we retrieved duration of functionality loss (flooding duration) and restoration duration from interviews with the homeowners. Using approximate estimation approach, loss values were assigned to each damaged entity. Functionality restoration models are developed using linear restoration models. The application of the proposed methodology is exemplified separately in the following sections.

3 Flood Vulnerability, Loss, and Recovery Models

3.1 Flood Vulnerability Models

Flood vulnerability models depict the expected mean DR under the given IM values in both univariate and multivariate formulations. DR up to 5% (0.05) indicates operational performance level even after flooding. A minimal investment is required for subsequent repair/restoration in this case. 5–15% DR signifies minor loss of functionality, but no significant damage–neither structural nor nonstructural. In this case, repair is required before 100% functionality can be restored. 15–30% DR outlines considerable loss of functionality and damage. Some parts of the entity require major repairs, so economic consequences will be significant in this case. However, the damage would be basically confined to nonstructural components. 30–50% DR indicates a major loss of functionality, which prompts the entity to be shut down for some time.

Major damage to important components of the entity is expected under this damage state. In this case, a significant amount should be invested to restore functionality. At this level, damage to structural components such as the load bearing walls, columns, etc. can also occur. 50–70% DR highlights extensive damage to the entity, and 100% functionality loss. Major rehabilitation to reconstruction/restoration of the entity is required to achieve 100% functionality. DR greater than 70% indicates a fully dysfunctional entity sustaining considerable structural damage or partial to complete collapse. The entire system should be restored/reconstructed to achieve 100% functionality. Implementing these damage and functionality loss schemes, the following section reports several sets of vulnerability, loss, and restoration models.

3.1.1 RC Buildings

Flood loading is lateral loading and RC frame constructions have better lateral load resistance capacity. Thus, inundation alone cannot damage structural components, such as beams, columns, slabs, and foundations in RC buildings. Under high flow velocity and extended flooding duration, RC foundation scouring can occur. Nonstructural components, such as infill walls, partition walls, boundary walls, and contents, are could be damaged by flood inundation. On the other hand, if significant momentum flux and debris impact excite RC buildings, detrimental consequences are also likely to occur (Gautam et al. 2023). Under low velocity flows, resulting in low momentum flux such as in mild and flat terrain rivers, nonstructural component damage can occur, for example, damage to infills, contents, warehouses, boundary walls, among others.

From the collected survey data, flood vulnerability surface for RC buildings is fitted using the RSM as shown in Fig. 2. Since our data does not contain collapsed RC buildings, and only a limited extent of inundation occurred during the two flooding scenarios, the peak DR value is only around 0.5. All the vulnerability models are constrained at the origin to ensure the boundary condition: —if there is no inundation, then the DR should be 0. It is seen in the figure that even low inundation depths for extended duration could result in DR of 0.1, whereas higher inundation depths abruptly increase DR.

Although bivariate vulnerability surfaces are superior models compared to univariate flood vulnerability models, flooding duration and inundation depth may not be always available simultaneously. Thus, we formulated univariate vulnerability models as well. These models would be ideally suitable if there is no information regarding the inundation duration. Figure 3 shows univariate flood vulnerability curve for RC buildings. The function can be used in flood loss assessment under probabilistic flooding scenarios for the given inundation depth associated with a return period.

3.1.2 Brick Masonry Buildings

Brick masonry construction does not have sufficient ductility under later loading, so damage can occur under high momentum flux. However, under low velocity flow, only scouring can be detrimental. Flood vulnerability surface for brick masonry buildings are plotted in Fig. 4. As shown in the figure, brick masonry buildings are more vulnerable than RC buildings under flood excitation as well. Even at low inundation depth with extended duration, DR could reach up to around 40%. On the other hand, higher inundation depth even for short duration could yield DR of up to 60%.

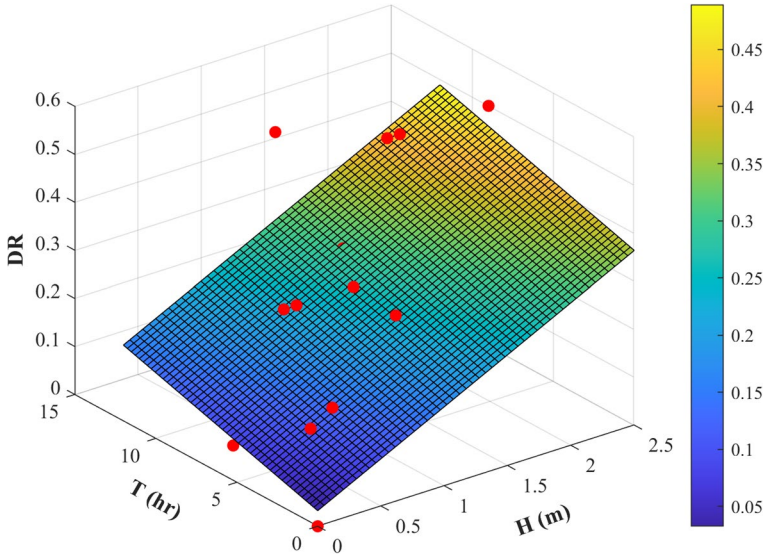

Fig. 2 Flood vulnerability surface for RC buildings. DR, T, and H respectively stand for damage ratio, inundation duration, and inundation depth. Red circles are the observed data

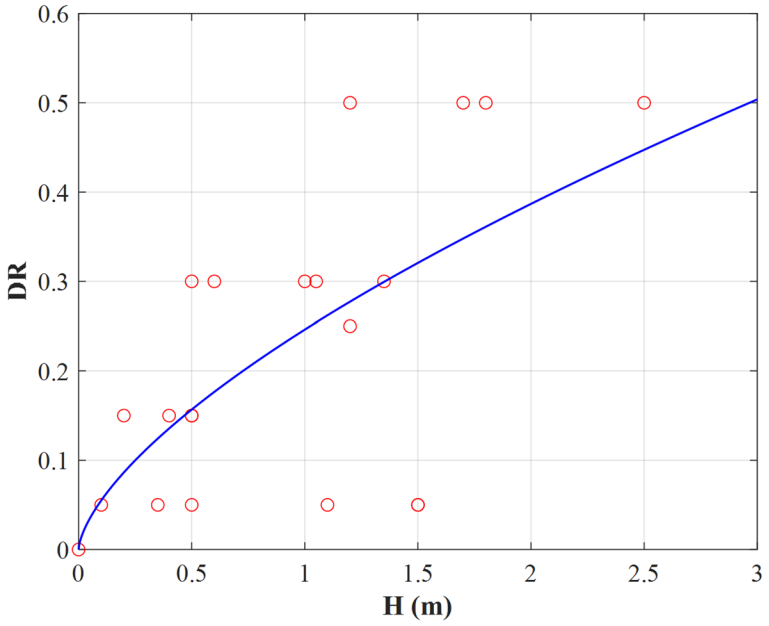

Fig. 3 Flood vulnerability function for RC buildings

Univariate flood vulnerability function for brick masonry buildings is shown in Fig. 5. At the inundation depth of around 3 m, brick masonry buildings are expected to observe DR of up to 100%. Figure 5 highlights that 100% DR is observed even at around 1.25 m inundation depth. This shows relatively uncertain flood performance of brick masonry buildings. For probabilistic flood risk assessments, the median vulnerability function is recommended.

3.1.3 Steel Buildings

Similar to RC buildings, steel buildings reflect considerable ductility, thus only a large momentum flux can trigger damage to structural components. Under low velocity flows, nonstructural components and contents can damage in steel buildings. Flood vulnerability surface for steel buildings is shown in Fig. 6. Under extended duration of low inundation depth, the maximum DR can reach up to 10%. Whereas, under extended inundation duration and high inundation depth, around 40% DR can be expected in steel buildings. It is important to note that an inundation depth of around 2 m for short duration is capable of yielding around 30% DR in steel buildings.

Univariate flood vulnerability function for steel buildings is shown in Fig. 7. Due to the lack of collapse and significant structural damage statistics, the vulnerability function is plotted only up to 40%. For higher DR, more data pertaining to higher damage states and associated inundation depth is required.

3.1.4 Semi-permanent Buildings

Semi-permanent buildings are usually constructed using steel frames and are used as periodic shop outlets, informal settlement, among others. Such buildings are not regulated con-

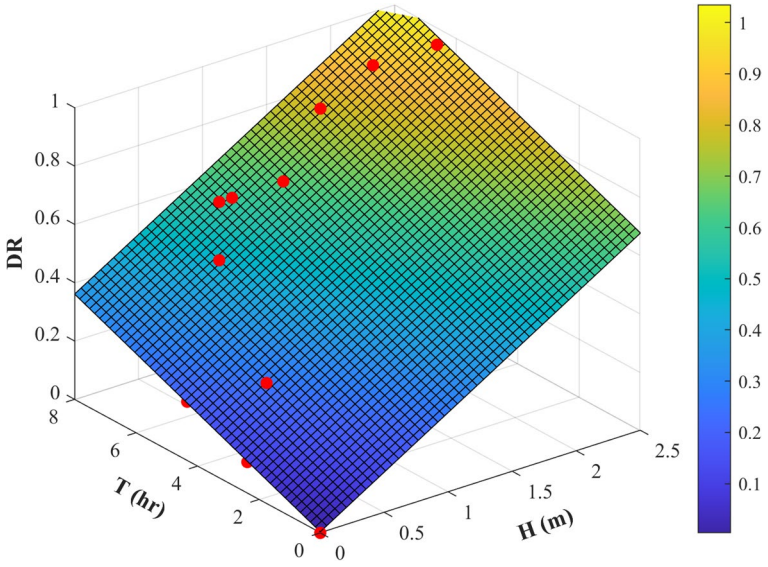

Fig. 4 Flood vulnerability surface for masonry buildings

structions, so a wide variety of these buildings can be found. Flood vulnerability surface for

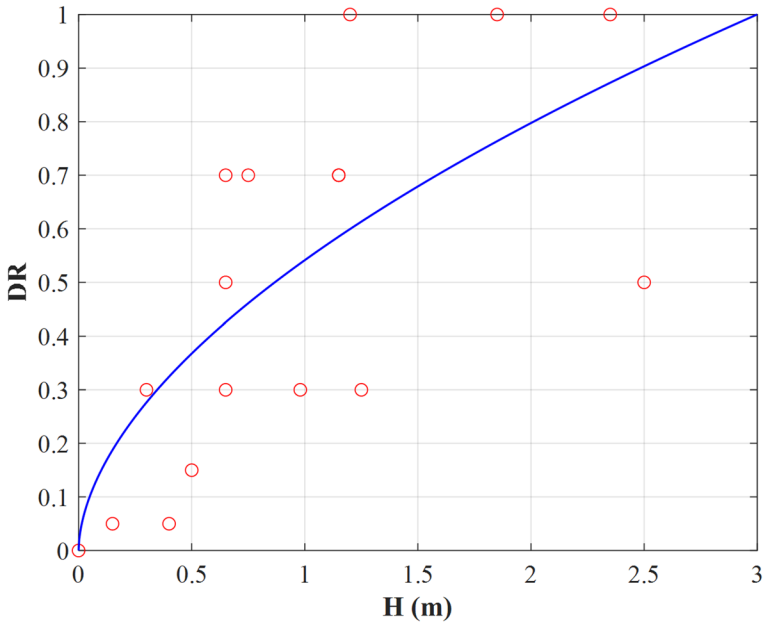

Fig. 5 Flood vulnerability function for brick masonry buildings

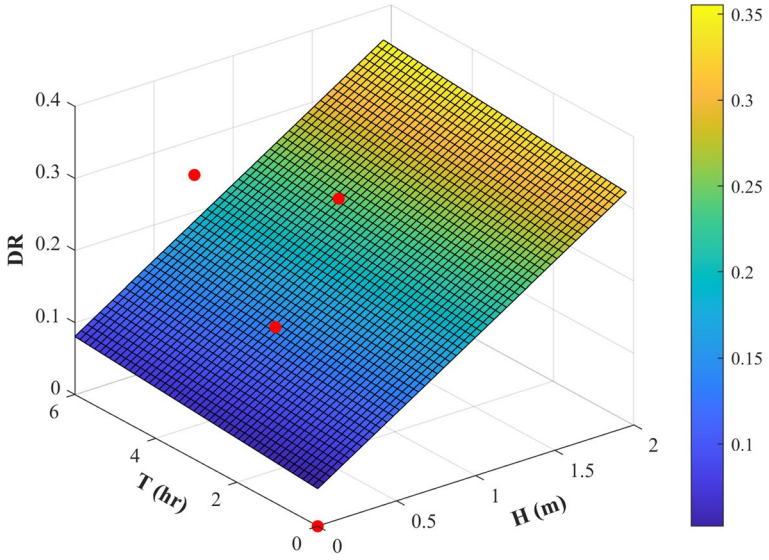

Fig. 6 Flood vulnerability surface for steel buildings

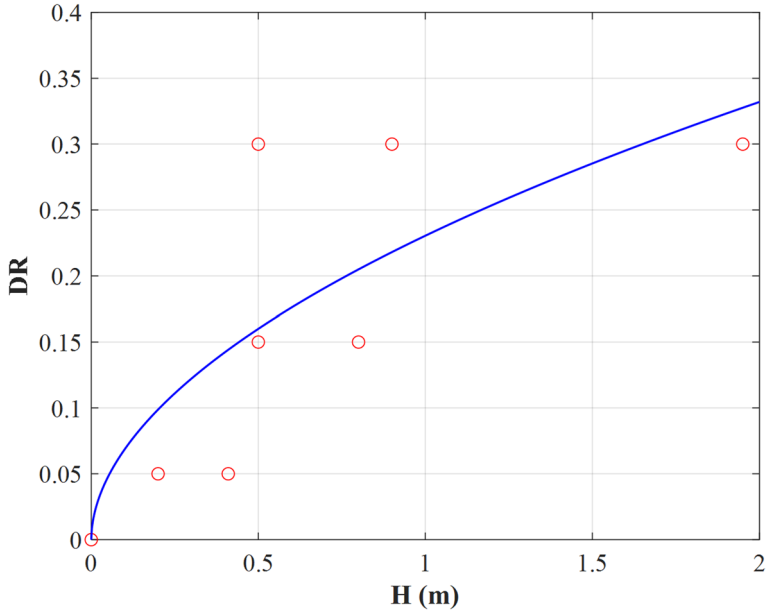

Fig. 7 Flood vulnerability function for steel buildings

semi-permanent buildings is shown in Fig. 8. Under extended duration and considerable inundation depth, DR of around 50% can be expected in such buildings. However, due to the lack of robust structural integrity and foundations, these buildings are susceptible to collapse if considerable momentum flux excites them.

Figure 9 shows the univariate flood vulnerability function for semi-permanent buildings. A 50% DR can be expected at around 1.5 m inundation depth. Meanwhile, DR rises up to 70% at 2 m inundation as shown in the figure.

3.1.5 Agricultural Land

Agricultural land is among the most affected entities by flooding within the built environment. Two types of crops, rice and corn, were covered during the field survey. Based on the crop type, crop maturity stage, resilience capacity with inundation duration, and size, the extent of damage can vary significantly. Flood vulnerability surface for agricultural land is shown in Fig. 10. The figure shows that inundation duration is the controlling factor for agriculture damage, rather than inundation depth. Under extended inundation hours, DR can reach up to 60% as shown in the figure. Although very effective, it is challenging to construct a flood vulnerability surface for agricultural land due to the inherent uncertainty pertaining to inundation depth determination. Unlike other entities within the built environment, the PFL estimation is not straightforward; thus, the model has inherent uncertainties too. We tried to develop a univariate flood vulnerability model for agricultural land, but the data did not constrain the model sufficiently. Hence, univariate flood vulnerability model is not reported.

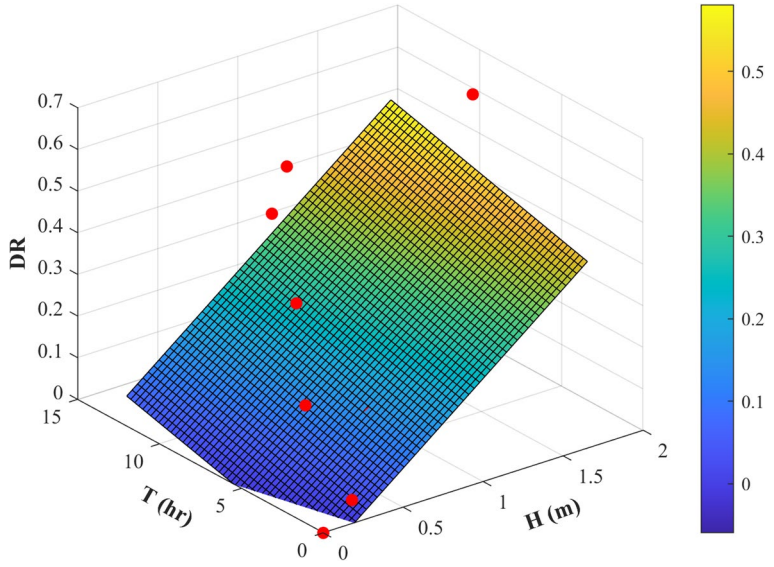

Fig. 8 Flood vulnerability surface for semi-permanent buildings

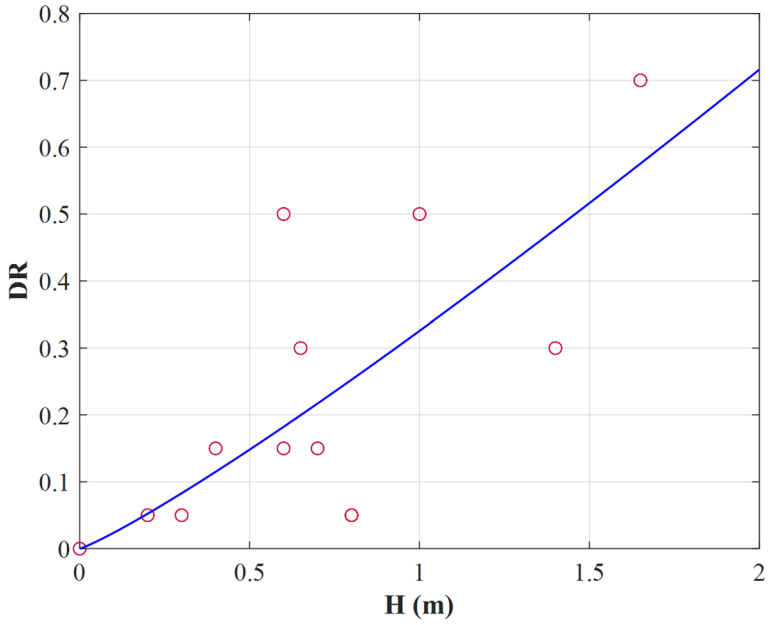

Fig. 9 Flood vulnerability function for semi-permanent buildings

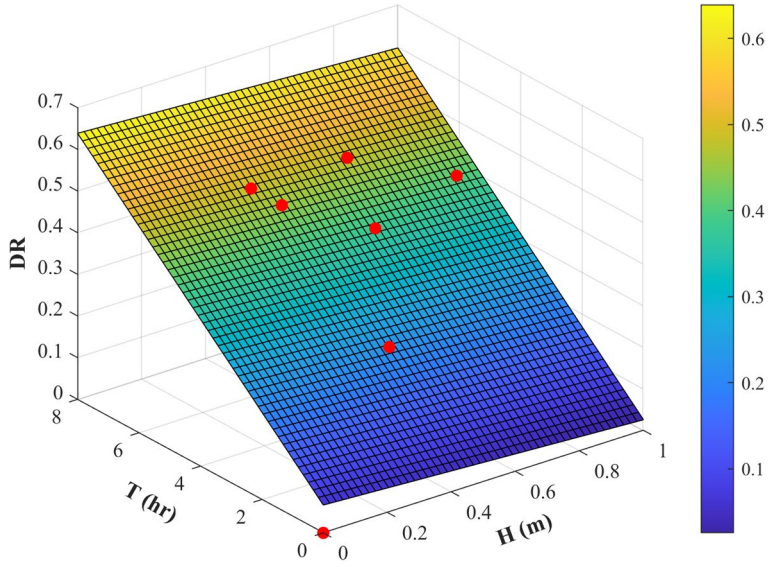

Fig. 10 Flood vulnerability surface for agricultural land

To estimate the equivalent loss, crop pattern, type, duration, resilience to flood inundation, and maturity stage of crops are the key factors. In addition, types of farming such as mixed or single cropping, cropping in furrow or in flat terrain etc. are also important to develop vulnerability and loss models. Future models can consider these dimensions to improve vulnerability and loss models.

3.2 Loss Models

Loss models depict straightforward information regarding the economic consequences of floods or any dynamic forces that incur damage to a particular entity. It is also possible to estimate the economic consequence using the ensemble of equivalent restoration values for each damaged component. However, the process is tedious because most of the damage assessment campaigns do not gather element by element damage data but rather focus on the global performance. Since we conducted structured surveys and captured total economic loss incurred by flood damage, we were able to construct loss surface and univariate loss model as detailed in the following sections.

3.2.1 RC Buildings

Flood loss surface for RC buildings is shown in Fig. 11. Considering inundation depth and DR, equivalent loss estimation model is developed. The loss values are from 2024, and any future use should consider inflation as well. Under 2.5 m inundation incurring DR of around 0.5, economic loss would be around US$ 5000 in RC buildings. However, there exists considerable uncertainty too. Under the low DR but high inundation depth, loss value can reach more than US$ 3000.

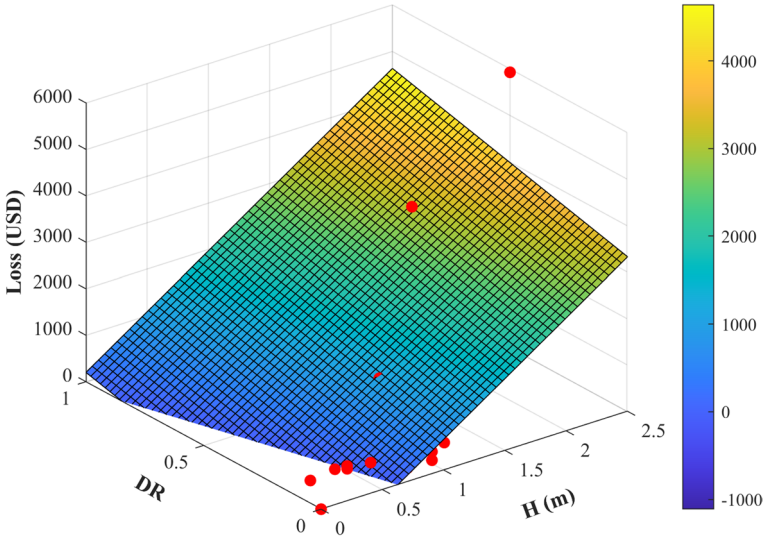

Fig. 11 Loss surface for RC buildings

Univariate loss model considering only inundation depth is shown in Fig. 12. The figure shows a good fit for the data; however, it might estimate equivalent loss even without the damage extent. So, the proposed loss function should be used cautiously. Particularly, the univariate loss model should be deployed to damaged RC buildings only. Up to 0.5 m inundation, no significant loss in RC buildings can be expected; however, a sharp increase can occur beyond 1.5 m of inundation depth.

3.2.2 Brick Masonry Buildings

Per unit loss incurred to brick masonry will be less than that in RC and steel constructions due to material cost. However, considerable losses can occur if DR is high even in brick masonry. Figure 13 shows loss surface for brick masonry buildings. At 1.5 m inundation and relatively low DR, loss value is expected to be less than US$ 1000 in brick masonry. However, if DR is high, loss value may reach up to US$ 2500. Due to significant interaction between the inundation depth and DR, we were not able to constrain the univariate loss model for brick masonry buildings.

3.2.3 Semi-permanent Buildings

Loss surface for semi-permanent buildings is shown in Fig. 14. Since semi-permanent buildings are low-cost constructions, associated losses will be lower than those for RC and other constructions. At 2 m inundation depth and low DR, loss value can reach up to US$ 1500. It is further interesting to note that loss value would not increase significantly for up to moderate damage extent. It is imperative to note that there are underlying uncertainties in the proposed model. More data can constrain the model better and downscale uncertainties.

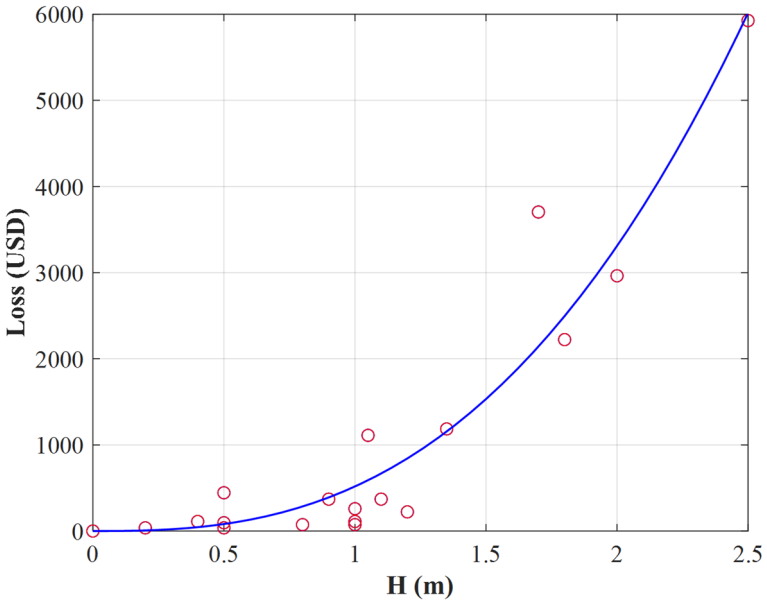

Fig. 12 Loss model for RC buildings

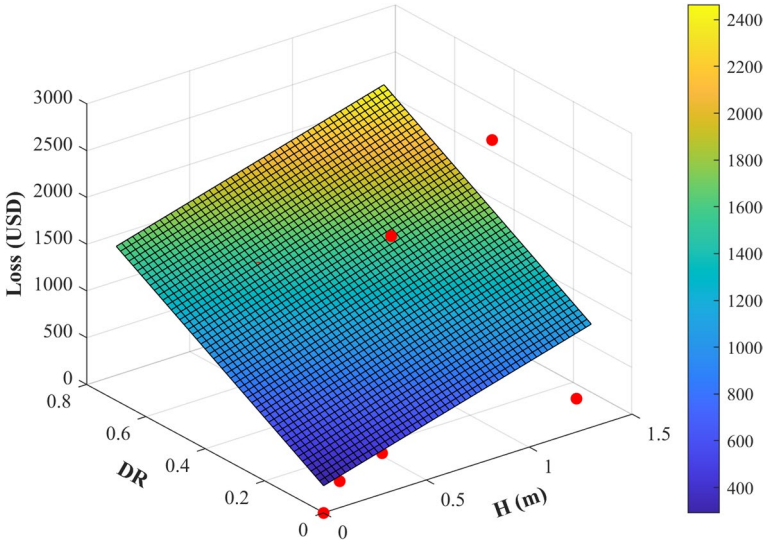

Fig. 13 Loss surface for masonry buildings

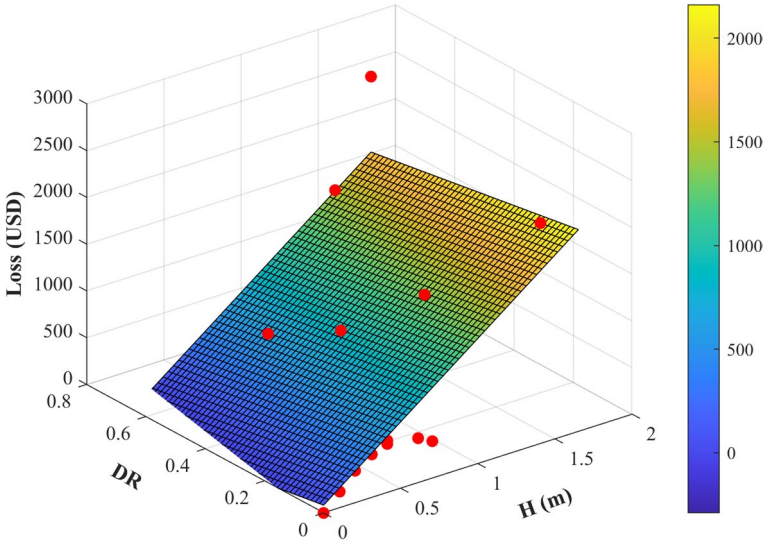

Fig. 14 Loss surface for semi-permanent buildings

3.3 Restoration Model

Unlike recovery models (Cimellaro et al. 2010), we propose restoration models, which pertain to the functionality restoration when damage ratio is usually low. Under significant damage, physical repairs/rehabilitation is required. This aspect will be better described under recovery modeling. On many occasions, flooding can cause water logging without any physical damage, and thus affects system functionality, but not structural integrity. In those cases, functionality restoration can be achieved using some resources as the entity would be still usable after some level of intervention. We propose a restoration model under usable damage state of any entity. Based on the recorded data, we were able to create restoration models for RC buildings only. When there is more than 15% of DR, the entity should follow a repair, which is often difficult to monitor because the models we proposed in this study comprise the damage/loss data from Kathmandu Valley where flood insurance is not practiced. In Kathmandu Valley, or in general in Nepal, people might opt not to repair, or may need time to save money to invest, or otherwise. To this end, constructing recovery models is not always straightforward. For the two functionality loss scenarios in RC buildings, restoration models are developed as shown in Fig. 15. Dashed lines in the figure represent the individual cases, whereas the bold lines are the mean models. It is evident that flooding occurred due to almost 2 h long torrential rain, so the initial 2 h are flat. Thereafter, the total duration of the HFL is considered to be around 0.5–1 h. Following that, a valley is formed until restoration is started. The length of the valley indicates the flooding duration (T) at which the stated functionality will be lost. After that, restoration efforts kick off and attain the top flat portion, indicating 100% functionality restoration. Functionality loss and restoration processes are assumed to be linear for both cases. We aim to extend these restoration models in the future using robust and well detailed database.

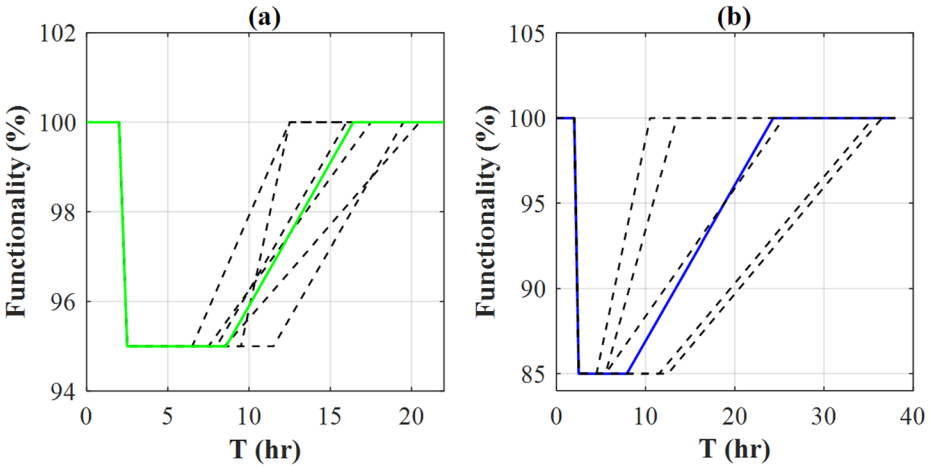

Fig. 15 Restoration models for RC buildings for: (**a**) slight functionality loss, (**b**) minor functionality loss. Dashed lines represent individual cases and bold green and blue lines are the average models

4 Application of the Models: Hybridization of Flood Hazard with Flood Impacts

Manohara River corridor in Kathmandu, Nepal (Fig. 16) is chosen as a case study implementation area, which witnessed massive flooding in August and September 2024 due to incessant rainfall occurring for two days. The availability of data required for validating the flood model and accessibility for field surveys were the other reasons for selecting the area. The Manohara River extends from 27^0 40' N to 27^0 42' N latitudes and 85^0 20' E to 85^0 22' E longitudes. Stretching 28 km from northeast to southwest, the Manohara watershed has the total area of 83 km^2 comprising straight upstream, which widens and meanders downstream. The same corridor has mixed formal and informal settlements and is known to be impacted by flooding almost every year. Due to the heterogeneous construction systems, the impacts are diffuse and so are the losses. Due to the lack of a flood insurance program, losses incurred to the built environment are at the stake of either owner or the government. Using the proposed vulnerability and loss models, a possible outlook could be the introduction of flood insurance in both government and private sector.

Traditional hydrological modeling techniques incorporating numerical methods that simulate rainfall-runoff phenomena are simple yet effective. Models such as HEC-RAS 2D with rain-on-grid facility have shown convincing performance on hydrological and flood inundation modeling over the years (Costabile et al. 2020). Modern approaches using neural networks such as Artificial Neural Networks (ANN) and Convolutional Neural Networks (CNN) have wider application in simulating hydrological response; however, adequate training data for acceptable accuracy would not be available in data scarce regions. Therefore, this study adopted HEC-RAS 2D for flood inundation modeling. It takes rainfall at multiple stations as an input and adjusts Manning's coefficient and infiltration values as per land cover type.

Data was pre-processed and fed into an event-based model developed in HEC-RAS 6.6 (https://www.hec.usace.army.mil/software/hec-ras/), incorporating both hydrologic and

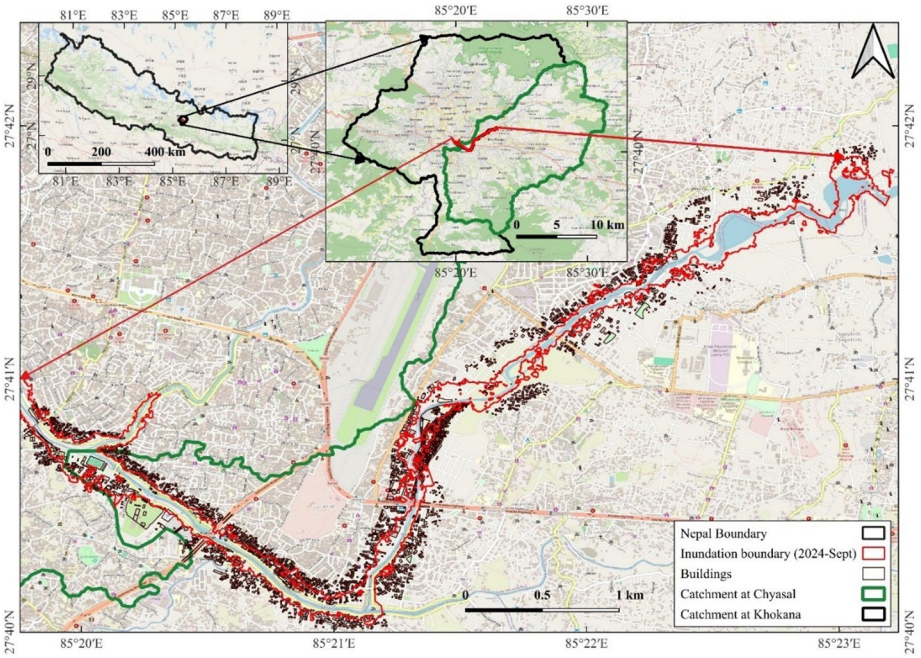

Fig. 16 Location and characteristics of the modeled area

hydrodynamic capabilities within a single user interface. A catchment-scale geometry was created in HEC-RAS with an outlet at Khokana station (see Fig. 16), and break lines were generated along the river profile with a mesh size of 30 × 30 m. The mesh size beyond the break lines was set to 300 × 300 m to minimize computational cost with normal depth boundary conditions assigned to the outlet. Precipitation gages were set on and around the geometry to input the observed rainfall data. A summary of input parameters and catchment detail is presented in Table 2. Further details regarding calibration and back analysis based validation of 2024 events are presented in the Appendix section.

Building shapefiles were extracted from the Open Street Map (OSM) consisting of the latest building footprints from the study area. The recent flood events were overlaid to the OSM base map and clipped using the respective flood inundation maps to obtain the number of inundated entities. The inundated entities are colored in light green for August 2024 (Fig. 22) and dark green for September 2024 (Fig. 23). For comparison, surveyed entities are marked in brown color.

The inundated entities are colored orange, purple, and red for floods of 5, 50, and 100-year return period (RP), consisting of 1244, 1452, and 1532 number of inundated entities, respectively. The three flooding scenarios are plotted in Fig. 24, Fig. 25, and Fig. 17, respectively. The inundation depths increased proportionately for successive RPs, with the maximum of 7.1 m for a 100-year RP. This indicates that a 100-year RP flooding will inundate at least two stories of a residential building. In this case, DR would exceed 60% even in RC buildings. To contextualize this with the 2024 flood, a site visit after the flooding revealed that almost all RC buildings in the flooded area withstood the flooding with considerable functionality loss only. It is pertinent to note that the 2024 flooding would fit between 5

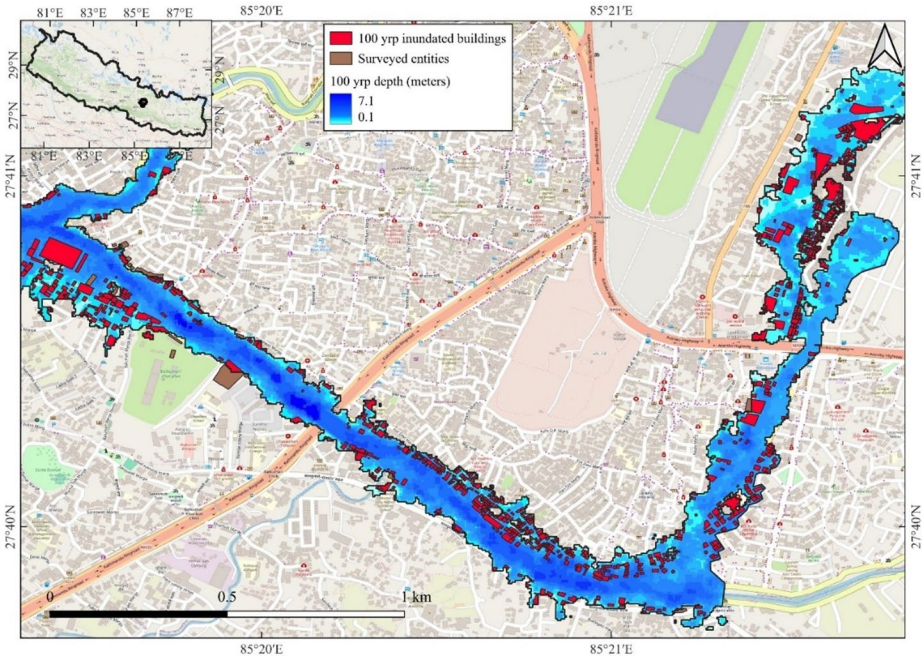

Fig. 17 Inundation map for 100-year RP flooding scenario

Fig. 18 **(a)** Functionality loss due to inundation and debris deposition in RC building, (**b**) an example of flood damaged semi-permanent building along the Manohara corridor, (**c**) damaged corn field by the 2024 flood

to 50-year RP but not 100-year RP. Evidently, the ground floor of all RC buildings in the affected areas inundated and got filled with debris, logs, and trash. Such an impact aligns toward functionality and economic losses rather than direct physical losses. An example of functionality loss in RC buildings is shown in Fig. 18. Although no direct physical damage is noted, the building required considerable amount to restore functionality. As shown in Fig. 24, even a 5-year RP flood would result in considerable inundation in the built environment. For any other inundation depth from another RP flooding, one can refer to respective vulnerability and loss models to quantify physical damage to economic consequences.

Inundation analysis depicted 1294 entities being inundated by the flood of September 2024. The value was greater than 5-year RP and slightly less than 50-year RP floods suggesting that the September flood aligns with the 50-year flood magnitude (Table 1). Consid-

Table 1 Number of entities inundated due to various scenario flooding

Scenario	Number of inundated entities in the built environment	Flooding area (km^2)	Remarks
August 2024 flood	924	0.98	
September 2024 flood	1294	1.4	>5 years RP to <50 years RP
5-year RP	1244	1.27	
50-year RP	1452	1.47	
100-year RP	1532	1.53	

ering the August 2024 flood as the base case, inundation was found to be 42.8% higher than that for the September 2024 flood. On the other hand, it was 29.6%, 50%, and 56.1% higher than that for 5, 50, and 100-year RP flooding, respectively.

The affected area has RC as the dominant form of residential construction. Although fewer buildings were exposed to the flood, brick masonry buildings also withstood the flooding event but sustained some level of functionality losses (Fig. 18a). Since inundation was limited in most cases, no considerable damage was noted, which adheres to the proposed flood vulnerability models. For the sake of brevity, field evidence on functionality losses in other building types are reported in this paper. No considerable physical damage was observed in steel buildings either. The results adhere to the proposed vulnerability models. Since most of the steel buildings were used for business purposes, training halls, and storage facilities, functionality losses were noted to be significant. This in turn yielded a considerable economic loss as well. Also, a significant amount of time and money had to be spent for restoring the functionality of the affected steel buildings. Along the river corridor, there were many semi-permanent buildings. Semi-permanent buildings sustained minor damage due to flooding, but remained functional as shown in Fig. 18b. Flood inundation caused significant losses and damage to food stocks, utensils, electrical equipment, etc., especially in semi-permanent buildings. Some of the agricultural lands present in the flooded area were significantly affected. Affected agricultural lands were covered with a thick layer of silt as shown in Fig. 18c. Corn fields were destroyed by the flood. Notably, construction of stone masonry walls of about 2 m height in some places controlled flood entry to the agricultural land. However, such countermeasures were not present throughout the river stretch.

5 Conclusions

Since flood impacts are highly dependent on the exposure and duration of flood inundation, univariate models for vulnerability and loss may not be explicitly representative. In order to account for this limitation and lay the foundation for multivariate flood vulnerability and loss assessment, we used response surface modeling, considering interaction between the intensity measures to create flood vulnerability and loss surfaces. Flood vulnerability and loss surfaces are also supplemented with univariate flood vulnerability and loss models for RC buildings, masonry buildings, steel buildings, and semi-permanent buildings. The models are developed using actual damage, inundation depth, and inundation duration data. The probabilistic models are compared and interpreted together with the probabilistic 2D flood hazard analysis in a case study region located in Kathmandu Valley, Nepal. We conclude that the existing flood hazard

modeling landscape can be extended to impact based approach, especially toward the built environment vulnerability, loss, and restoration. The proposed models can be deployed to another region with similar construction systems, such as south and southeast Asian regions. However, inundation depth limits should be marked before adopting the models for other regions. In addition, Bayesian updating can be performed using data from different settings to develop generalized and representative models for transregional applications. In flood prone areas such as the Manohara River corridor in Kathmandu, even a 5-year RP flood can cause significant functionality loss together with considerable economic consequences, although robust construction systems such as RC and steel buildings do not necessarily observe physical damage. Meanwhile, the restoration model developed in this study concludes that functionality restoration may require considerable time (>15 h) even in the case of slight to minor functionality losses. This indicates that indirect losses are significant in every kind of structural system. This aspect is often overlooked; however, the models developed in this study reflect that it cannot be overlooked in flood prone areas. Due to the lack of interdisciplinary efforts, flood vulnerability, economic loss, and restoration models are extremely rare in the literature. Meanwhile, we conclude that a deeper understanding of flood impact in the built environment requires streamlined and coordinated efforts from multiple disciplines, including water resources, hydrology, hydraulic, geology, and structural engineering, to develop reliable and high-fidelity models. The flood vulnerability and loss models can be used in flood insurance planning, flood-resistant construction system development, flood strengthening of structures, and other purposes. If both inundation depth and inundation duration cannot be retrieved simultaneously, univariate functions can be used, which is the most common practice as of now. Future studies can consider updating the models proposed in this study when additional data from empirical, experimental, or numerical analysis become available. In addition, bias treatment and uncertainty quantification can be considered in future studies. Also, there is an opportunity to cover more building forms, infrastructures, and other components of the built environment. Another important consideration in the future is the adoption of hydrodynamic and impact forces in damage depiction. If velocity is available at each entity, momentum flux can be used as an IM instead of inundation depth alone. The vulnerability model for agricultural land is a preliminary model and thus requires an update in the future considering crop resilience, different stages of crops, crop types, and multi-crop scenarios within the affected areas.

Appendix

Table 2 summarizes the input and sources used for hydrologic modeling. Precipitation records and river discharge were collected from the Department of Hydrology and Meteorology (DHM), Government of Nepal. The records include daily time series cumulative rainfall (mm) covering the watershed, and average daily discharge (m^3/s) data at Khokana station (Station Index: 550.05) between 1995 and 2024. Additionally, the rating curve and stage readings at Manohara station (Station Index: 538) during recent flooding (August/September 2024) were also acquired for validation. Geospatial data such as digital elevation model (DEM) and land use/cover (LULC) were required for both HEC-RAS and HEC-HMS models. We used TerraSAR-X add-on for DEM (TanDEM-X) distributed by the Earth Observation Center (EOC) of German Aerospace Center (https://download.geoservice.dlr.de/TDM30_EDEM/). The LULC map was extracted from the Sentinel open access site (ht

Table 2 Characteristics of the study area used for flood hazard modeling

Data Type	Resolution		Source
	Spatial	Temporal	
DEM	5 m (resampled)	2015	TanDEM-X
LULC map	10 m (resampled)	2020	ICIMOD (href="https://www.icimod.org/" data-mce-href="https://www.icimod.org/">https://www.icimod.org/)
Rainfall	Daily/sub daily	1995 – 2024	DHM
Discharge	Daily/sub daily	1995 – 2024	DHM

tps://livingatlas.arcgis.com/landcoverexplorer/#mapCenter=-66.80083%2 C-9.32196%2C11&mode=step&timeExtent=2017%2C2023&year=2023).

Contrary to the hydrologic modeling approach, which can simulate time series rainfall-runoff phenomenon, a hydrodynamic model can emulate peak flood events more accurately for short term event-based simulations. The event-based calibration, performed using trial-and-error procedure, showed acceptable performance with parameter sets shown in Table 3. Fig. 19 and Fig. 20 respectively demonstrate the model's capability to reproduce the historical flood events of 2002 and 2004 with acceptable performance.

The calibrated model was applied to simulate the recent flood of August/September 2024 to validate the model. Simulated discharge at Manohara station was compared with the discharge computed using the rating curve from DHM. The model is found to be capable of reproducing the recent flood event of August 2024 reasonably well as shown in Fig. 21.

Furthermore, inundation depth along the Manohara River is mapped using the HEC-RAS model and real-time observations have been added to validate the map. The simulated depths were comparable with the observed depths collected from the field survey. It showed Nash-Sutcliffe Efficiency (NSE) and R^2 of 0.88 and 0.94, respectively for August 2024

Table 3 Final set of parameters used for HEC-RAS calibration

Land cover type	Manning's parameter		Infiltration parameter		
	Manning's n	% imperviousness	Maximum deficit (mm)	Initial deficit (mm)	Potential percolation rate (mm/hr)
Waterbody	0.065	45	10	5	0.02
Snow	0.0001	100	0	0	0.0001
Forest	0.08	15	15	10	0.35
Riverbed	0.065	55	15	10	0.3
Built up area	0.11	80	10	7	0.1
Cropland	0.04	10	15	10	0.25
Bare soil	0.045	10	15	10	0.45
Bare rock	0.05	25	10	5	0.1
Grassland	0.055	15	20	15	0.45
Other wooded land	0.065	10	15	10	0.1

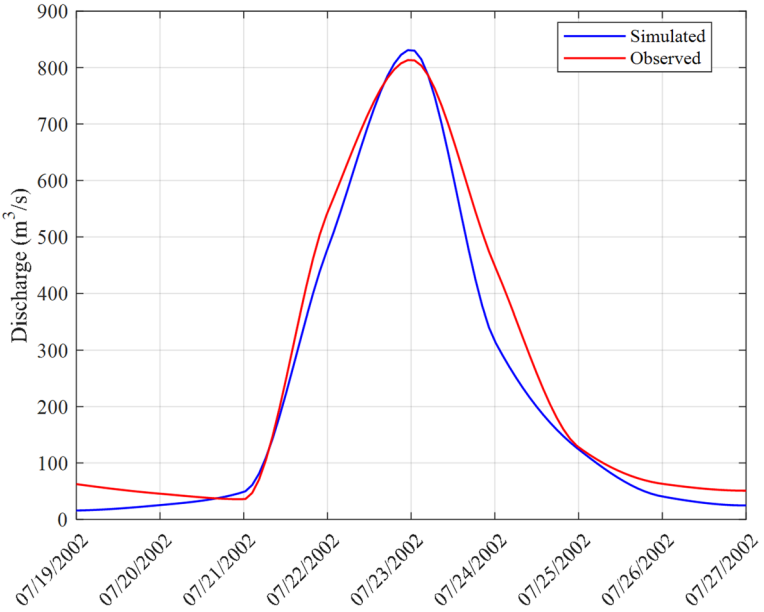

Fig. 19 Calibration of HEC-RAS model at Khokana hydrological station for 2002 flood event

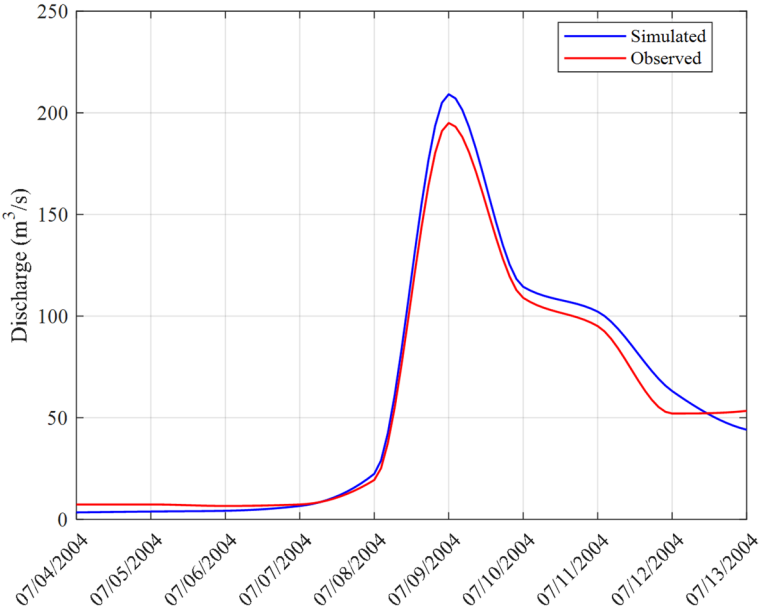

Fig. 20 Calibration of HEC-RAS model at Khokana hydrological station for 2004 flood event

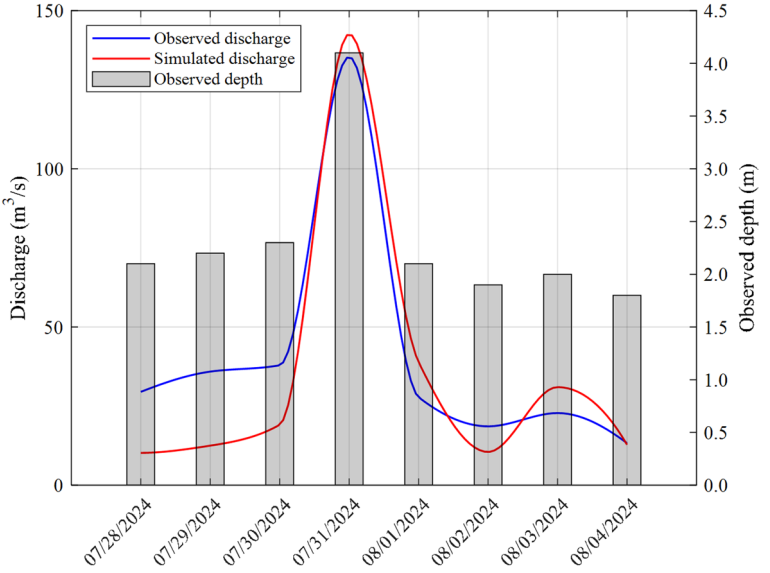

Fig. 21 Comparison between estimated discharge based on the observed water level and rating curve and HEC-RAS simulated discharge at Manohara station for August 2024 flood event

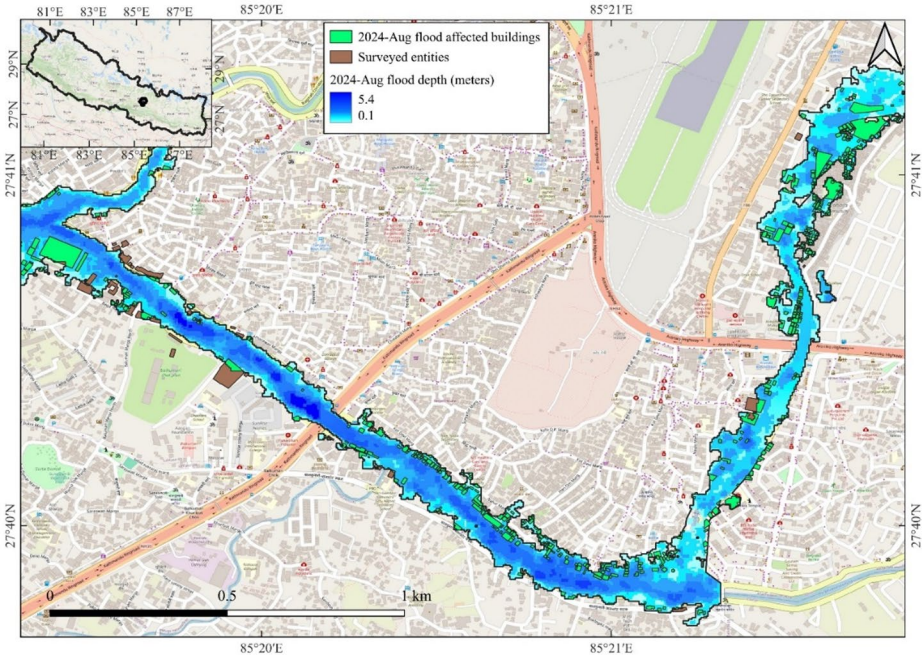

Fig. 22 Inundation mapping for 2024 August flood

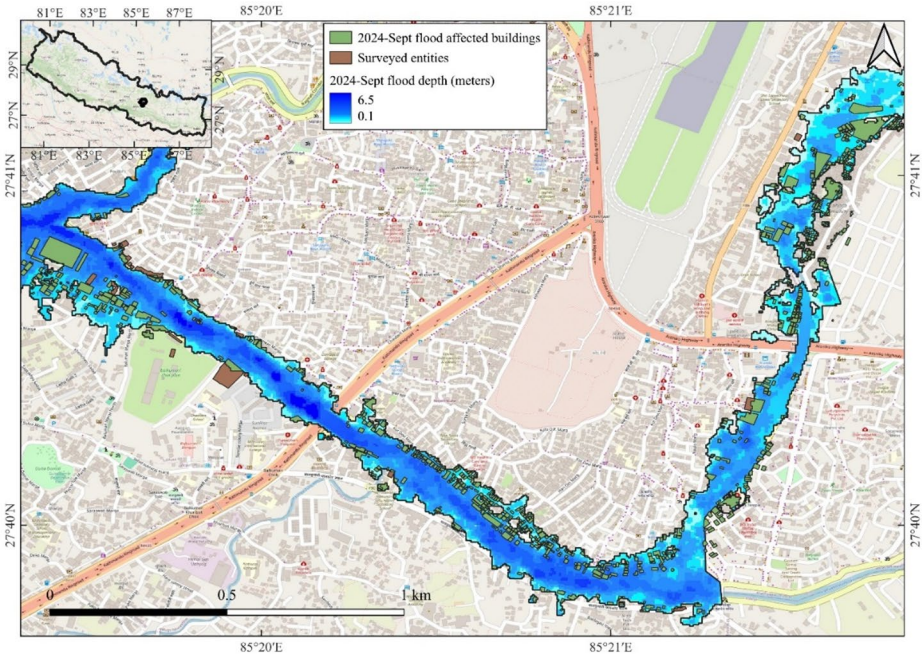

Fig. 23 Inundation mapping for 2024 September flood

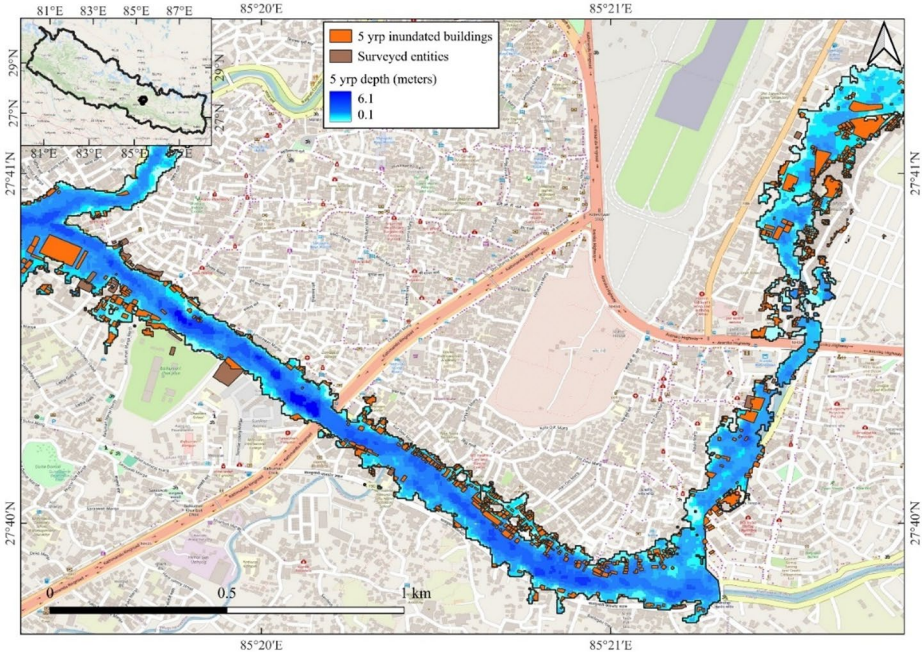

Fig. 24 Inundation map for 5-year RP flooding scenario

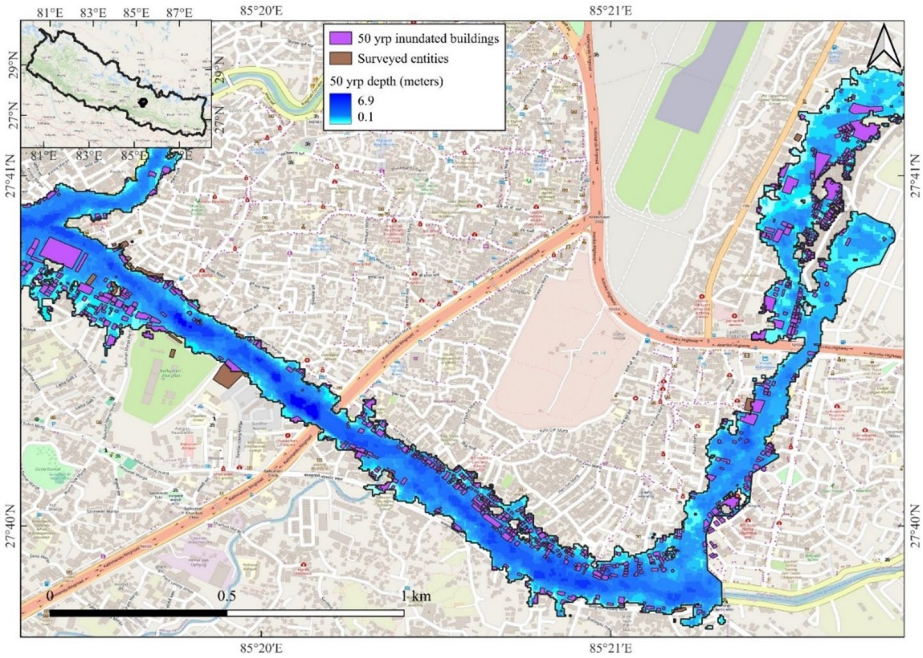

Fig. 25 Inundation map for 50-year RP flooding scenario

flood, and 0.94 and 0.95, respectively for September 2024 flood. Strong positive coefficient of determination validates the representativeness of the numerical model.

After calibrating the HEC-RAS model, the parameter sets were transferred to the HEC-HMS model to estimate historical time series at Manohara station. The outcome was then used for flood frequency analysis using Gumbel's method at Manohara station. Water levels and flood inundation maps were generated from HEC-RAS for the August 2024, and September 2024 flood events as well as various return period floods. The maps were post-processed using QGIS.

After calibration and validation of the historical events, rainfall frequency analysis at individual rainfall stations was carried out using Gumbel's method to extrapolate rainfall values for different return periods. The rainfall values were input to the calibrated model at the respective gages to simulate flooding adhering to different return periods.

Funding Open access funding provided by Università degli Studi di Napoli Federico II within the CRUI-CARE Agreement. The authors declare that no funds, grants, or other support were received during the preparation of this manuscript.

Declarations

Competing interests The authors have no relevant financial or non-financial interests to disclose.

References

Amirmoradi K, Shokoohi A (2024) River flash flood economical loss and its uncertainty in developing countries. Water Resour Manage 38:81–105. https://doi.org/10.1007/s11269-023-03653-3

Arrighi C, Mazzanti B, Pistone F, Castelli F (2020) Empirical flash flood vulnerability functions for residential buildings. SN Appl Sci 2(5):904. https://doi.org/10.1007/s42452-020-2696-1

Bangalore M, Hallegatte S, Vogt-Schilb A, Rozenberg J (2017) Unbreakable: Building the Resilience of the Poor in the Face of Natural Disasters. In *Unbreakable: Building the Resilience of the Poor in the Face of Natural Disasters*. https://doi.org/10.1596/978-1-4648-1003-9

Cheng S, Yang M, Li C, Xu H, Chen C, Shu D, Jiang Y, Gui Y, Dong N (2024) An improved coupled hydrologic-hydrodynamic model for urban flood simulations under varied scenarios. Water Resour Manage 38(14):5523–5539. https://doi.org/10.1007/s11269-024-03914-9

Cimellaro GP, Reinhorn AM, Bruneau M (2010) Seismic resilience of a hospital system. Struct Infrastruct Eng 6(1–2):127–144. https://doi.org/10.1080/15732470802663847

Costabile P, Costanzo C, Ferraro D, Macchione F, Petaccia G (2020) Performances of the new HEC-RAS version 5 for 2-D hydrodynamic-based rainfall-runoff simulations at basin scale: comparison with a state-of-the art model. Water (Switzerland) 12(9):2326. https://doi.org/10.3390/W12092326

de Moraes RBF, Gonçalves FV (2024) Development, application, and validation of the urban flood susceptibility index. Water Resour Manage 38(7):2511–2525. https://doi.org/10.1007/s11269-024-03782-3

De Risi R, Jalayer F, De Paola F, Carozza S, Yonas N, Giugni M, Gasparini P (2020) From flood risk mapping toward reducing vulnerability: the case of Addis Ababa. Nat Hazards 100(1):387–415. https://doi.org/10.1007/s11069-019-03817-8

Forte G, De Falco M, Santo A, Gautam D, Santangelo N (2025) Flash flood impacts and vulnerability mapping at catchment scale: insights from the Southern Apennines. Eng Geol 350:107988. https://doi.org/10.1016/j.enggeo.2025.107988

Fuchs S, Heiser M, Schlögl M, Zischg A, Papathoma-Köhle M, Keiler M (2019) Short communication: a model to predict flood loss in mountain areas. Environ Model Softw 117:176–180. https://doi.org/10.1016/j.envsoft.2019.03.026

Fuchs S, Keiler M, Ortlepp R, Schinke R, Papathoma-Köhle M (2019) Recent advances in vulnerability assessment for the built environment exposed to torrential hazards: challenges and the way forward. J Hydrol 575:587–595. https://doi.org/10.1016/j.jhydrol.2019.05.067

Gautam D, Dong Y (2018) Multi-hazard vulnerability of structures and lifelines due to the 2015 Gorkha earthquake and 2017 central Nepal flash flood. J Build Eng 17:196–201. https://doi.org/10.1016/j.jobe.2018.02.016

Gautam D, Fabbrocino G, de Santucci Magistris F (2018) Derive empirical fragility functions for Nepali residential buildings. Eng Struct 171:617–628. https://doi.org/10.1016/j.engstruct.2018.06.018

Gautam D, Adhikari R, Gautam S, Pandey VP, Thapa BR, Lamichhane S, Talchabhadel R, Thapa S, Niraula S, Aryal KR, Lamsal P, Bastola S, Sah SK, Subedi SK, Puri B, Kandel B, Sapkota P, Rupakhety R (2023) Unzipping flood vulnerability and functionality loss: tale of struggle for existence of riparian buildings. Nat Hazards 119:989–1009. https://doi.org/10.1007/s11069-022-05433-5

Jang JH, Vohnicky P, Kuo YL (2021) Improvement of flood risk analysis via downscaling of hazard and vulnerability maps. Water Resour Manage 35:2215–2230. https://doi.org/10.1007/s11269-021-02836-0

Karagiorgos K, Thaler T, Heiser M, Hübl J, Fuchs S (2016) Integrated flash flood vulnerability assessment: insights from East Attica, Greece. J Hydrol 541:553–562. https://doi.org/10.1016/j.jhydrol.2016.02.052

Mascheri G, Chieffo N, Arrighi C, Del Gaudio C, Lourenço PB (2024) A framework for multi-risk assessment in a historical area of Lisbon. Int J Disaster Risk Reduct 108:104508. https://doi.org/10.1016/j.ijdrr.2024.104508

Molinari D, Rita Scorzini A, Arrighi C, Carisi F, Castelli F, Domeneghetti A, Gallazzi A, Galliani M, Grelot F, Kellermann P, Kreibich H, Mohor GS, Mosimann M, Natho S, Richert C, Schroeter K, Thieken AH, Paul Zischg A, Ballio F (2020) Are flood damage models converging to "reality"? Lessons learnt from a blind test. Nat Hazards Earth Syst Sci 20(11):2997–3017. https://doi.org/10.5194/nhess-20-2997-2020

Panagiotou CF, Feloni E, Aristidou K, Eliades M (2025) Probabilistic assessment of flood susceptibility via a coparticipative multicriteria decision analysis. Environ Processes 12:22. https://doi.org/10.1007/s40710-025-00766-2

Papathoma-Köhle M, Gems B, Sturm M, Fuchs S (2017) Matrices, curves and indicators: a review of approaches to assess physical vulnerability to debris flows. Earth Sci Rev 171:272–288. https://doi.org/10.1016/j.earscirev.2017.06.007

Papathoma-Köhle M, Schlögl M, Dosser L, Roesch F, Borga M, Erlicher M, Keiler M, Fuchs S (2022) Physical vulnerability to dynamic flooding: vulnerability curves and vulnerability indices. J Hydrol 607:127501. https://doi.org/10.1016/j.jhydrol.2022.127501

Pistrika A, Tsakiris G, Nalbantis I (2014) Flood depth-damage functions for built environment. Environ Processes 1(4):553–572. https://doi.org/10.1007/s40710-014-0038-2

Rentschler J, Salhab M, Jafino BA (2022) Flood exposure and poverty in 188 countries. Nat Commun 13:3527. https://doi.org/10.1038/s41467-022-30727-4

Santangelo N, Forte G, De Falco M, Chirico GB, Santo A (2021) New insights on rainfall triggering flow-like landslides and flash floods in Campania (Southern Italy). Landslides 18:2923–2933. https://doi.org/10.1007/s10346-021-01667-9

Santo A, Santangelo N, Forte G, De Falco M (2016) Post flash flood survey: the 14th and 15th october 2015 event in the paupisi-Solopaca area (Southern Italy). J Maps 13(2):19–25. https://doi.org/10.1080/17445647.2016.1249034

Santo A, Di Crescenzo G, Forte G, Papa R, Pirone M, Urciuoli G (2018) Flow-type landslides in pyroclastic soils on flysch bedrock in southern Italy: the Bosco de' Preti case study. Landslides 15:63–82. https://doi.org/10.1007/s10346-017-0854-3

Sturm M, Gems B, Keller F, Mazzorana B, Fuchs S, Papathoma-Köhle M, Aufleger M (2018) Experimental analyses of impact forces on buildings exposed to fluvial hazards. J Hydrol 565:1–13. https://doi.org/10.1016/j.jhydrol.2018.07.070

Taramelli A, Righini M, Valentini E, Alfieri L, Gatti I, Gabellani S (2022) Building-scale flood loss estimation through vulnerability pattern characterization: application to an urban flood in Milan, Italy. Nat Hazards Earth Syst Sci 22(11):3543–3569. https://doi.org/10.5194/nhess-22-3543-2022

Thapa S, Shrestha A, Lamichhane S, Adhikari R, Gautam D (2020) Catchment-scale flood hazard mapping and flood vulnerability analysis of residential buildings: the case of Khando River in eastern Nepal. J Hydrol Reg Stud 30:100704. https://doi.org/10.1016/j.ejrh.2020.100704

Totschnig R, Fuchs S (2013) Mountain torrents: quantifying vulnerability and assessing uncertainties. Eng Geol 155:31–44. https://doi.org/10.1016/j.enggeo.2012.12.019

Authors and Affiliations

Vishnu Prasad Pandey[1,2] · Pradhumna Joshi[1] · Rabindra Adhikari[3] · Bhesh Raj Thapa[4] · Sabin Dangol[1] · Ashish Devkota[1] · Aayush Gautam[1] · Giovanni Forte[5] · Dipendra Gautam[6]

✉ Giovanni Forte
giovanni.forte@unina.it

✉ Dipendra Gautam
dipendra.gautam@unimol.it

[1] Center for Water Resources Studies, Institute of Engineering, Tribhuvan University, Kirtipur, Nepal

[2] Department of Civil Engineering, Pulchowk Campus, Institute of Engineering, Tribhuvan University, Kirtipur, Nepal

[3] Department of Civil Engineering, Cosmos College of Management and Technology, Lalitpur, Nepal

[4] Department of Civil Engineering, Universal Engineering and Science College, Lalitpur, Nepal

[5] DICEA, Dipartimento d'Ingegneria Civile, Edile e Ambientale, Università degli Studi di Napoli Federico II, Via Claudio 21, Napoli 80125, Italy

[6] Faculty of Civil and Environmental Engineering, University of Iceland, Reykjavik, Iceland